



Contents lists available at Egyptian Knowledge Bank

Microbial Biosystems

Journal homepage: <http://mb.journals.ekb.eg/>

Preparation of nanocomposite based on zinc oxide nanoparticles and biopolymers: Characterization, antimicrobial and anticancer activities

Nady Saber Mohamed Alnagar¹, Mohamed Hasanin^{2,3}, Waleed B. Suleiman¹, Shimaa A. Zaki⁴, Amr H. Hashem^{1*}

¹ Botany and Microbiology Department, Faculty of Science, Al-Azhar University, Cairo-11884, Egypt.

² Cellulose and Paper Department, National Research Centre, El-Buhouth St., Dokki, 12622, Egypt.

³ Department of Polymer and Biomaterials Science, West Pomeranian University of Technology in Szczecin, Al. Piastow 45, 70-311 Szczecin, Poland.

⁴ Plant Pathology Research Institute, Agricultural Research Centre, 12619, Giza, Egypt.



ARTICLE INFO

Article history

Received 1 October 2024

Received revised 20 November 2024

Accepted 30 January 2025

Available online 1 March 2025

Corresponding Editors

El-Sayyad, G. S.

AbdElgawad, H.

Keywords

Antibacterial and anticancer properties, biocompatibility, cytotoxicity, drug delivery, green synthesis of nanoparticles.

ABSTRACT

In the current study, zinc oxide nanoparticles (ZnONPs) were successfully mycosynthesized using *Rhizopus arrhizus* NWMA1 and formulated into carboxymethyl cellulose (CMC) and starch (ST) as nanocomposite (CMC/St@ZnONPs). The ZnONPs and formulated CMC/St@ZnONPs were characterized physiochemically and topographically as well. ZnONPs UV-visible spectrum presented a peak at 270 nm. Additionally, the Fourier transform infrared (FTIR) of CMC/St@ZnONPs emphasized the formulation. Moreover, X-ray diffraction (XRD) diffraction of ZnONPs and CMC/St@ZnONPs were presented in the crystal plane of ZnONPs that decreased after formulation according to the effect of biopolymers. The topographical analysis including transmission electron microscopy (TEM), selected area electronic diffraction (SAED), scanning electron microscopy (SEM) and energy dispersive X-ray (EDX) affirmed the formulation of ZnONPs and incorporation of ZnONPs into CMC/St@ZnONPs. The prepared compounds were assessed for antimicrobial activity toward multi-drug resistant bacterial and fungal isolates as well as for anticancer activity toward MCF7 cancerous cell line. Antimicrobial results revealed that CMC/St@ZnONPs nanocomposite showed activity higher than ZnONPs where inhibition zones were 40, 25, 43, 17, 25, 25, 25 and 45 mm against *K. pneumonia* 124, *K. pneumonia* 117, *B. subtilis*, *K. pneumonia* 115, *Acinetobacter baumannii* 110, *Pseudomonas aeruginosa*, *E. coli* 127, *C. albicans*. Furthermore, ZnONPs exhibited anticancer activity higher than CMC/St@ZnONPs nanocomposite toward MCF7 cells where IC₅₀ was 61.22 ± 1.09, and 84.47 ± 2.48 μg mL⁻¹ respectively. In conclusion, this study succeeded in the mycosynthesis of ZnONPs and CMC/St@ZnONPs nanocomposite which had promising antimicrobial and anticancer activity.

Published by Arab Society for Fungal Conservation

*Corresponding author Email address: amr.hosny86@azhar.edu.eg (Amr H. Hashem)



Introduction

The rise of multidrug-resistant (MDR) microbes presents significant risks to public health, leading to increased morbidity and mortality rates. Infections caused by these resistant strains often result in prolonged hospital stays, higher medical costs, and the necessity for more intensive care (Kumar et al. 2024). Patients undergoing surgeries, cancer treatments, or organ transplants are particularly vulnerable, as they rely heavily on effective antibiotics to prevent and treat infections. The inability to treat common infections effectively can lead to complications that may ultimately result in death, creating a pressing need for new therapeutic options (Hocking et al. 2021). Moreover, the spread of MDR microbes poses a broader risk to healthcare systems and society at large. Outbreaks of resistant infections can overwhelm healthcare facilities, leading to resource scarcity and increased strain on healthcare professionals (Salam et al. 2023). Additionally, the economic burden extends beyond individual patients to entire communities and countries, as the costs associated with treatment, hospitalization, and lost productivity can be substantial. Public health efforts are further challenged by the global nature of drug resistance, as resistant strains can easily spread across borders, necessitating coordinated international responses to effectively address this growing crisis (Muteeb & Rehman 2023).

Cancer poses significant risks not only to individual patients but also to public health systems and society as a whole. The disease can lead to severe physical, emotional, and financial burdens for patients and their families (Więckiewicz et al. 2024). The prognosis for cancer can vary widely depending on the type and stage at diagnosis, with some cancers being highly treatable while others remain difficult to manage. Late-stage diagnoses often result in more aggressive treatments, which can be physically taxing and may lead to long-term health complications (Neal et al. 2015). On a broader scale, the prevalence of cancer contributes to significant economic challenges, including high healthcare costs and lost productivity (Cong et al. 2022). Cancer treatment often requires extensive resources, including surgeries, chemotherapy, radiation, and ongoing follow-up care, leading to substantial financial strain on healthcare systems. Moreover, as the population ages and lifestyle factors such as smoking, poor diet, and lack of exercise contribute to rising cancer rates, the burden on public health initiatives grows (Smith et al. 2019). This necessitates concerted efforts in prevention, early detection, and treatment strategies to mitigate the risks associated with cancer and improve outcomes for affected individuals and communities.

Over the last decade, nanotechnology has emerged as a technology that has revolutionized every field of applied science. The field of nanoparticles (NPs) is one of the avenues to nanotechnology that is associated with nanoscale materials with very small particles size ranging from 1 to 100 nm. In this regard, NPs have been integrated into various industries by providing innovative solutions (Saied et al. 2022, El-Khawaga et al. 2023). Therefore, it can be incorporated into various applications such as textiles, wastewater treatment, paper preservation, the food industry, cosmetics and pharmaceuticals, optics, and smart devices (Albalawi et al. 2022, Hashem et al. 2023a, Hashem & El-Sayyad 2024). Biological synthesis or green synthesis has been described as cost-effectiveness, biocompatible, eco-friendly nature, and scalable, avoiding harsh conditions and not utilizing hazardous chemicals. Various biological entities such as bacteria, fungi, yeast, actinomycetes, and plant extracts are utilized in the green synthesis of different metal and metal oxide nanoparticles, such as Ag, Cu, CuO, ZnO, TiO₂, Se, and Fe₂O₃ (Abdel-Azeem et al. 2020; Srivastava et al. 2021; Al-Askar et al. 2023, Hashem et al. 2023b, Saied et al. 2023, Gaber et al. 2024).

ZnONPs are characterized as being efficient against pathogenic microorganisms, mostly by their antimicrobial properties according to their photo-oxidizing and photocatalytic (Hashem et al. 2023 c, d; Elkady et al. 2024). Recently detailed reviews introduced the preparation methods and antifungal properties of ZnONPs and their possible antifungal mechanisms for plant diseases management and to improve food quality (Zaki et al. 2021).

Polysaccharides play a role in nanoparticle formulation and synthesis (Hasanin and Youssef 2022, Hasanin et al. 2023c, Samir et al. 2024). The formulation of nanoparticles maintains stability and prevents particle aggregations (Shrestha et al. 2020). Cellulose and its derivatives have unique characteristics such as biodegradability, compatibility and many of these materials are edible as well (Elsayed et al. 2022, Hasanin et al. 2023a). Carboxymethyl cellulose (CMC) is a water-soluble cellulose derivative that is edible.

Moreover, CMC recognized for its biodegradable and biocompatible properties, presents several advantages that position it as a promising biomaterial for pharmaceutical and biomedical applications (Pourmadadi et al. 2023). For example, its advantages include affordability, non-toxicity, and bioavailability (Almajidi et al. 2023).

On the other hand, starch has outstanding biocompatibility, complete degradability without toxic residues, cost-effectiveness, broad availability, and edible and renewable characteristics, which present numerous opportunities in biomedical applications,

including bone tissue engineering and drug delivery systems (Hasanin 2021, Kader et al. 2024).

Starch is a biopolymer used as a composite with CMC for nanoparticle formulation and green synthesis sometimes (Gopinath et al. 2022). The combination of CMC biopolymer and ZnONPs to composite has better mechanical properties and chemical stability. Zinc oxide nanoparticles can be used as nanofillers have antimicrobial activity, nontoxicity, improved mechanical properties of nanocomposites, and a synergistic effect on antimicrobial properties with biopolymers (Ponco et al. 2020, Youssef et al. 2020). The current study aimed to: (1) myco-synthesize ZnONPs and CMC/St@ZnONPs composite, using an easy, eco-friendly, environmentally safe and costless approach, employing fungal metabolites from *Rhizopus arrhizus* as a reducing agent and stabilizer to synthesize ZnONPs. (2) Characterize the prepared ZnONPs and CMC/St@ZnONPs composite to confirm synthesis, structure, size and NPs morphology using UV-Vis spectroscopy and TEM, SEM-EDX, XRD, and FTIR analyses. (3) Assess the *in vitro* antimicrobial activity against multi-drug resistant bacterial as well as anticancer activity at safe concentrations.

Materials and methods

Materials

In the current study, zinc acetate (Molecular Biology Grade, Merck, Kenilworth, NJ, USA). Methanol and sodium hydroxide (NaOH) were used as analytical grades and obtained from Sigma Aldrich, Cairo, Egypt. The potato dextrose agar medium (PDA) (Sigma–Aldrich, St., Louis, MO, USA). Mueller-Hinton agar medium (Oxoid, Cairo, Egypt). Carboxymethyl cellulose sodium salt (CMC) (Mw = 700,000 g/mol, Ds = 0.9, and starch (Sigma-Aldrich, Cairo, Egypt). All biological reactions were carried out using distilled water.

Methods

Isolation and identification of fungal isolate

Fungal isolate was isolated from soil sample from Giza Governorate by direct method where plated on malt extract agar (MEA) (Merck, Germany) medium plates, and incubated at 28 ± 2 °C for 3-4 days. Various colonies of different morphologies were individually picked off and replicated on MEA plates and then kept at 4 °C for further use (Fouda et al. 2015, Hashem et al. 2019, Hasanin et al. 2020). Morphological identification of the fungus was carried out by observing the morphological characteristics (color, texture, and appearance) and microscopic characteristics using light microscope (Khalil & Hashem 2018, Khalil et al. 2019, Hashem et al. 2020a,b). DNA was extracted from agar cultures using Quick-DNA Fungal/Bacterial Microprep Kit (Zymo research; D6007)

following the manufacturer's protocol and supported by Sigma Scientific Services Company (Egypt). PCR was performed by using Maxima Hot Start PCR Master Mix (Thermo; K1051). The primers used were Forward ITS1-F (5'- TCCGTAGGTGAACCTGCGG-3') and Reverse ITS4-R (5'- TCCTCCGCTTATTGATATGC-3') according to method used by Visagie et al. (2014).

Synthesis of zinc oxide nanoparticles

Biosynthesis of ZnONPs was carried out according to our previous work with minor modifications (Abu-Elghait et al. 2021). *Rhizopus arrhizus* NWMA1 was cultured on Malt extract broth (MEB) medium (Biolab, Hungary) at 30°C, 150 rpm for 7 days. Filtration was carried out using Whatman filter paper No. 1 to obtain cell-free filtrate. The filtrate was used for ZnONPs synthesis as follows: 1 mM of Zinc acetate was added to cell free filtrate of *R. arrhizus* and incubated at 30°C for 24h on shaker 150 rpm.

Preparation of CMC/St@ZnONPs

Firstly, 2 g of CMC was dissolved in 100 mL distilled water, and magnetic stirred until completely dissolved. In another beaker, prepare a starch solution by dissolving 1 g of starch in distilled water (50 mL) with constant stirring in a magnetic stirrer. The blended solution was obtained by adding CMC and starch in a 2:1 (w/w) ratio, and by continued stirring (10 min), 0.5 g of ZnONPs was added to the mixture under steering at 1500 rpm for 1 h then sonication to mix. Then the mix was precipitated with an equal volume of absolute methanol. The precipitate was filtrated and washed by methanol two times then washed with deionized water and preserved in a refrigerator to further investigations (Jiang et al. 2020).

Characterizations

UV-visible spectroscopy was carried out using UV-visible spectrophotometer (T80 uv/visb spectrophotometer pg instruments ltd) absorption spectra were measured between 0 and 600 nm. As a blank, distilled water was used. X-ray diffraction (XRD) analysis was used to examine the structure of powder nanoparticles. Cu K α radiation ($\lambda = 1.54$ Å) was used in the scattering range (2θ) of 0–80° at a scan rate of 0.03S1 on a D8 Advance X-ray diffractometer (Bruker). As an internal standard for calibration, a standard silicon sample was used. Fourier transform infrared (FTIR) of the type Bruker VERTEX 80v spectrometer. Transmission electron microscopy (TEM) micrographs were taken on a Carl Zeiss Leo 912 AB OMEGA electron microscope at an accelerating voltage of 80 kV as well as the selected area electronic diffraction (SAED). Scanning electron microscopy (SEM) coupled with energy dispersive X-ray analysis; Model Quanta 250 FEG (Field Emission Gun) attached with EDX

Unit (Energy Dispersive X-ray Analyses) for EDX. Samples were mounted on aluminum microscopy stubs using carbon tape, then coated with gold (Au) for 120 s using Quorum Techniques Ltd, sputter coater (Q150t, England).

Test microorganisms

Bacterial strains were provided from patient specimens (urine, sputum, and blood) at Sayed Galal Hospital, which were clinically identified by the VITEK[®] 2 and subsequently investigated for their susceptibilities to different 20 antibiotics discs according to agar disc diffusion method described by (Shawky et al. 2021). Additionally, *Candida albicans* was investigated for its susceptibility to the selected antibiotic list, and then the multidrug-resistant strains were assessed and reported.

Antimicrobial activity

The antimicrobial activity of ZnONPs and CMC/St@ZnONPs composite was assessed using the agar plate-diffusion method against various multi-drug resistant bacterial and fungal isolates. To check antimicrobial activity, each isolate was homogeneously streaked over Mueller-Hinton agar (for bacterial strains) and PDA plates (for *C. albicans*) using a sterilized cotton swab. Three wells (0.7 cm diameter) were cut in the streaked Mueller-Hinton plates and filled with 100 μ L of biosynthesized ZnONPs, CMC/St@ZnONPs composite, and zinc acetate (1000 μ g mL⁻¹). The results were recorded as a zone of inhibitions (ZOIs) around each well by mm. The experiment was achieved in triplicate (Hasanin et al. 2023b).

Cytotoxic Activity of ZnONPs and CMC/Starch@ZnONPs toward normal and cancerous cell lines

Cytotoxicity

The cytotoxicity of ZnONPs and CMC/St@ZnONPs composite was determined using the MTT protocol (Van de Loosdrecht et al. 1994) with minor modifications. The normal Vero cells and Cancerous MCF7 cell lines were collected from American type culture collection (ATCC). The cell quantity and the percentage of viable cell were totaled by the following formula:

$$\text{Viability \%} = \frac{\text{Test OD}}{\text{Control OD}} \times 100$$

$$\text{Inhibition \%} = 100 - \text{Viability \%}$$

Statistical analyses

Three replicates were done, and all resulting values are the averages of three independent experiments. Data was analyzed using a one-way ANOVA model of analysis of variance (ANOVA) ($\alpha=0.05$) to determine the significance

between groups. When significance differs was detected by pairwise comparisons, multiple comparisons were performed using Tukey's test.

Results and discussion

Identification of the fungal isolate for biosynthesis of ZnONPs

Morphological identification of fungal isolates

A fungal isolate of NWMA 1 was isolated and identified morphologically and genetically. Colonies of fungal isolate are fast growing and a dark white with faint black in color, sporangiophores are brownish and branched, and sporangia are spherical in shape, black in color, and large in size. Sporangiospores are oval in shape (Figure 1).

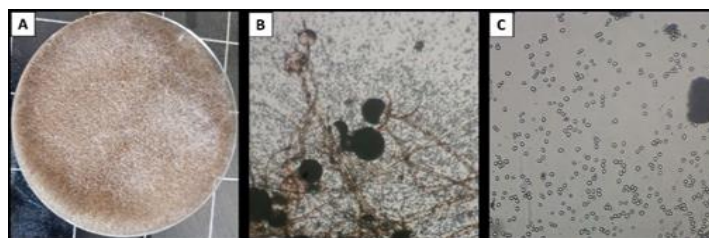


Fig 1. *Rhizopus arrhizus* (NWMA1), A- colony, B- sporangia and sporangiophores and C- sporangiospores.

To confirm the morphological identification, A fungal isolate was identified genetically using the ITS region. The sequence analysis revealed that the fungal NWMA1 was highly related to *Rhizopus arrhizus* (accession number PQ270498.1) with similarity percentages of 99.31 %. Therefore, the fungal isolate NWMA1 in this study was specifically identified as *Rhizopus arrhizus* isolate NWMA1 as shown in the phylogenetic tree (Figure 2). The molecular identification confirmed the morphological identification of *R. arrhizus*, and this sequence was deposited in a gene bank with accession number PQ203973.1.

Characterizations

UV-Visible spectroscopy

Figure 3 illustrates the UV-visible spectroscopy spectrum of the mycosynthesis of ZnONPs using NWMA1 isolate. The spectra showed absorbance peaks around 270 nm, which correspond to the characteristic band of ZnONPs, according to previous notices (López & Rodriguez-Paez 2017, Karam & Abdulrahman 2022).

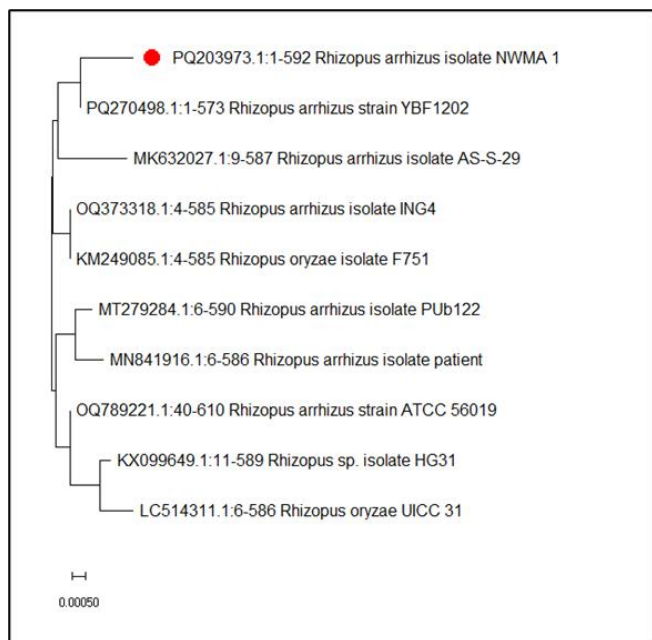


Fig 2. Phylogenetic tree of the fungal taxon *Rhizopus arrhizus* (NWMA1).

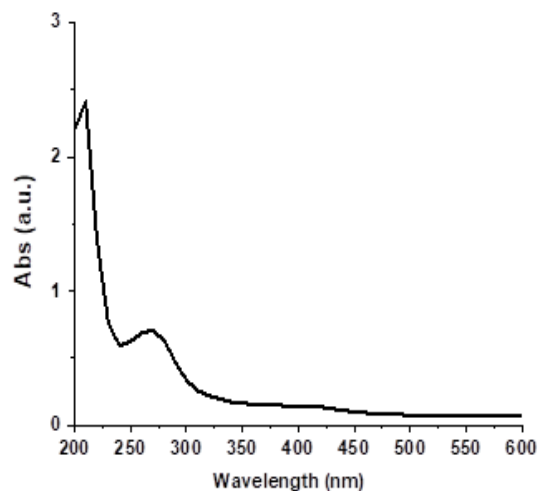


Fig 3. UV-Vis spectrum of ZnONPs produced by NWMA1.

The XRD patterns of synthesized zinc oxide nanoparticles using NWMA1 isolate shown in Figure 4A. The diffraction pattern observed peaks located at 31.84° , 34.52° , 36.33° , 47.63° , 56.71° , 62.96° , 68.13° , 69.18° , 70.16° , 73.21° , and 78.56° which ascribed to the (100), (002), (101), (102), (110), (103), (200), (112), (201) (004), and (202) planes, respectively. The obtained peaks can be indexed to the hexagonal wurtzite structure of ZnO (JCPDS card no. 36–1451) (Kim et al. 2017, Reddy et al. 2017). On the other side, the CMC/ST@ZnONPs matrix diffraction patterns (Figure 4B) display a broad peak at 2θ equal to around 23° that is associated with the low

crystallinity of the CMC/St polysaccharide template structure in addition to the diffraction peaks of ZnO located at 31.84° , 34.52° , 36.33° , 47.63° , 56.71° , 62.96° , 68.13° , 69.18° , 70.16° , 73.21° , and 78.56° corresponding to the hexagonal wurtzite structure of ZnO (JCPDS card no. 36–1451). These observations affirmed the formulation of ZnONPs into the CMC/ST template.

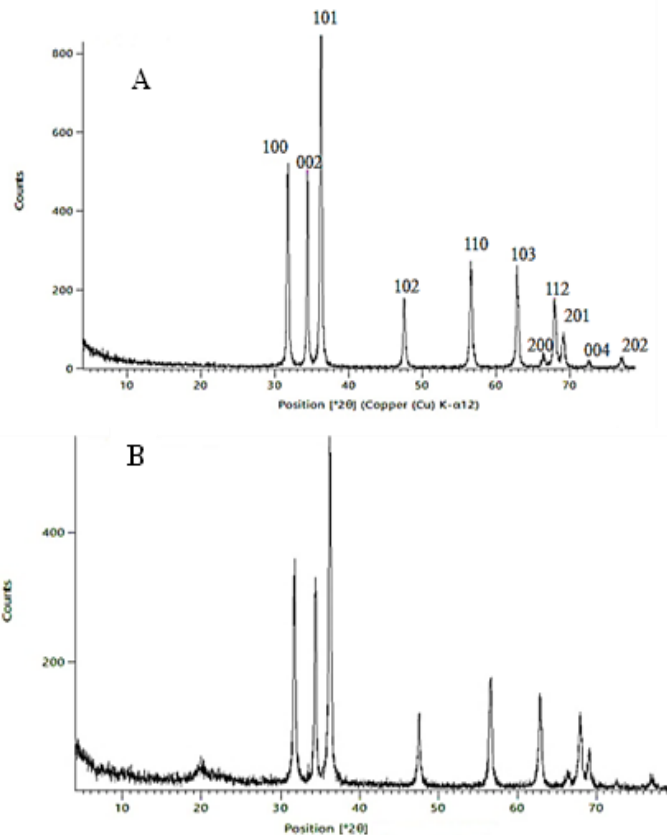


Fig 4. X-ray diffraction pattern of ZnONPs of NWMA1 (A) and nanocomposite (B).

FTIR spectroscopy spectrum of CMC/ST@ZnONPs composite synthesized by NWMA1 isolate was presented in figure 5. FTIR measurements were carried out to identify the potential functional groups of the molecules present in the nanocomposite. Metal oxides generally give absorption in the fingerprint region, i.e., below 1000 cm^{-1} , arising from inter-atomic vibrations. In this context, the bands at 626 and 561 cm^{-1} corresponded to Zn-O stretching and hexagonal phase ZnO, respectively (Kumar & Rani 2013). These affirmed the formulation of the ZnONPs into nanocomposite. In addition, the band at 2921 cm^{-1} corresponds to the C-H stretch, and the band at 3860 cm^{-1} corresponds to OH stretching vibration, all

representing the polysaccharides (Abdelraof et al. 2020, Hasanin et al. 2022). The band at 1409 cm^{-1} due to interactions between ZnO nanoparticles and the O-H groups. 1324 cm^{-1} corresponds to C-H bending (Soubhagya et al. 2022). Moreover, the band at 1135 cm^{-1} corresponds to the C-O-C carbohydrate linkage (Turky et al. 2020, Hasanin 2021). These above findings affirmed the formulation of CMC/ST@ZnONPs.

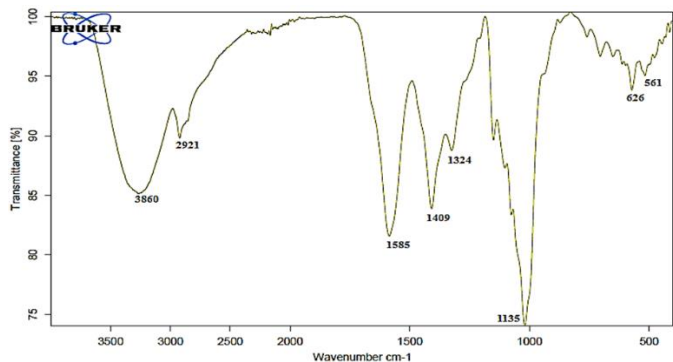


Fig 5. FTIR spectrum of CMC/ST@ZnONPs synthesized by NWMA1 isolate.

Topographical analysis

The topographical analysis, including TEM and SEM with EDX charts, was carried out to study the size and shape of biosynthesis ZnONPs using NWMA1 isolate. TEM images showed a mixture of hexagonal and spherical, shaped particles for the ZnONPs nanoparticles synthesized (Figure 6 A). Particle size was within the ranges of 8-25 and 6-15 nm. The nanoparticles were individuals and agglomerated in clusters. Diffraction rings can be allocated as (100), (002), and (101) planes from the SAED pattern of ZnONPs (Figure 6 B), representing the hexagonal structure coupled with the wurtzite-like structure of ZnONPs as shown in the XRD pattern (Ruddaraju et al. 2019, Zaki et al. 2021). In addition, the CMC/ST@ZnONPs TEM image presented in (Figure 6C) is a nanonetwork that could be referred to as CMC and ST, as well as many black dots were observed on the surface due to the ZnONPs particles. Additionally, the SAED pattern (Figure 6D) was presented with low crystallinity compared to ZnONPs that returned to the interaction of CMC and ST.

In addition, SEM images and EDX chart of CMC/ST@ZnONPs ZnONPs by NWMA1 isolate is presented in Figure (7). The low magnification SEM image observed a rough surface with some spots of metallic chain due to polysaccharides and ZnONPs, respectively. On the other side, the high magnification SEM image (Figure 7 B) was presented as a fluffy surface that due to the structure of the biopolymer that doped with metallic spherical shapes continuous

homogeneity, crack-free, and bubble-free morphology on the surface can be seen. The EDX chart of CMC/ST@ZnONPs (Figure 7C) revealed a Zn-specific peak around 1 keV and a weak signal at about 8.5 keV, which was characteristic absorption for metallic Zn, also peaks of carbon oxygen and nitrogen are seen, evidencing the presence of CMC as capping agent that increases the relative concentrations of carbon and sodium.

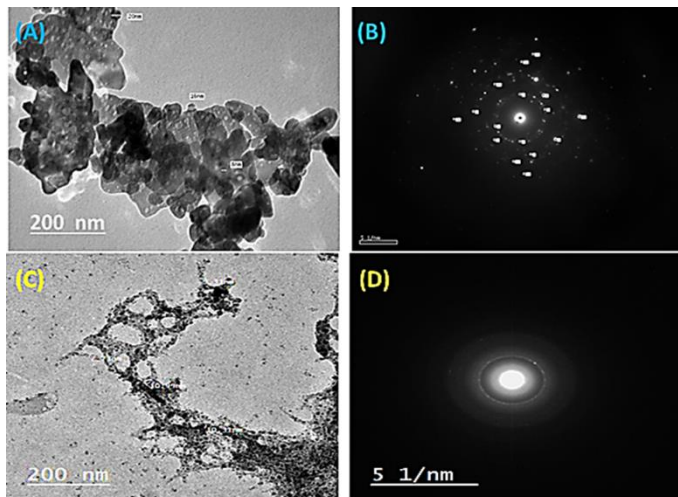


Fig 6. TEM images of synthesized ZnONPs synthesized by NWMA1 isolate (A), SAED of ZnONPs. TEM images of synthesized CMC/ST@ZnONPs (C) and SAED (D).

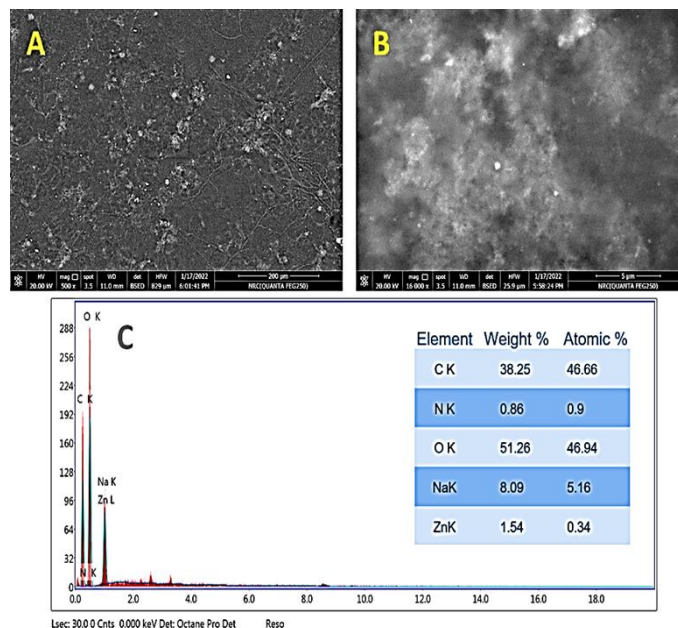


Fig 7. SEM images at different magnifications at low (A) and high (B) of CMC/ST@ZnONPs as well as EDX chart (D).

Isolation and identification of pathogenic bacteria

Thirty pathogenic bacteria were recovered from different patient specimens, and VITEK® 2 was used for clinical identification, Table 1 describes the pathogenic bacterial strains, and their percentage ascendingly ordered. *Candida albicans* as a unicellular fungus in addition to 9 pure bacterial cultures was recovered once with a percentage of (3.33%); *Aeromonas veronii*, *Bacillus subtilis*, *Citrobacter youngae*, *Klebsiella ozaenae*, *Proteus mirabilis*, *Pseudomonas aeruginosa*, *Pseudomonas fluorescens*, *Serratia marcescens*, and *Staphylococcus heamolyticus*. Two cultures of *Enterobacter cloacae* were isolated with a percentage of (6.67%). Three cultures of *Acinetobacter baumannii* were purified and their percentage represents (10%). Five cultures of *E. coli* which represent 16.67%, and 10 pure cultures of *Klebsiella pneumonia* (33.33%) were also reported.

An antibiotic susceptibility test was performed, and the multidrug-resistant strains were selected. Accordingly, their assessment report was tabulated in Table 2 that describes the antibiotic susceptibility profiles of the MDR and as well as their index which indicates degree of susceptibility of each selected strain depending upon MIC values according to CLSI 2010, 2011 (Kamel et al. 2022, Soliman et al. 2022).

Out of the 30 isolated bacterial strains, 8 MDR strains were selected for further investigations; *Acinetobacter baumannii* 110, *Bacillus subtilis*, *E. coli* 127, *Klebsiella pneumonia* 115, 117, 124, and *Pseudomonas aeruginosa*. Table 2 shows *Acinetobacter baumannii* 110 was the most resistant strain. In contrast, it showed resistance to all 20 tested antibiotics followed by *Klebsiella pneumonia* 124 and *Pseudomonas aeruginosa* which were resistant to 19 tested antibiotics and only susceptible to tigeccycline. On the other hand, *E. coli* 127 was

susceptible to 4 antibiotics: amikacin, gentamycin, nitrofurantoin, and tigeccycline.

Antimicrobial activity of ZnONPs and CMC/St@ZnONPs composite

Nanocomposites have emerged as promising materials in the field of antimicrobial applications due to their enhanced surface area and unique properties (Hasanin et al. 2021, Hasanin et al. 2022, Saravanan et al. 2023). By incorporating nanoparticles, such as silver, copper, or zinc oxide, into a polymer matrix, these nanocomposites exhibit superior antimicrobial activity against a wide range of pathogens (Elbasuney et al. 2021, Shehabeldine et al. 2022).

In this study, the antimicrobial activity ZnONPs, CMC/St@ZnONPs composite and $Zn(CH_3COO)_2 \cdot 2H_2O$ solution were tested at concentration of $1000 \mu g mL^{-1}$ using agar diffusion method. Seven bacterial strains (*K. pneumonia* 127, *K. pneumonia* 117, *B. subtilis*, *K. pneumonia* 115, *Acinetobacter baumannii* 110, *Pseudomonas aeruginosa* and *E.coli* 127, in addition to the unicellular fungus *C. albicans*) were used as shown in Tabl 3 and Figure 8. Results revealed that, ZnONPs exhibited antibacterial and antifungal activity toward multidrug-resistant bacteria and fungi where Inhibition zones toward *K. pneumonia* 124, *K. pneumonia* 117, *B.subtilis*, *K. pneumonia*115, *Acinetobacter bumanii* 110, *pseudomonas aerogenosa*, *E. coli* 127, *C. albicans* were 28, 21, 36, 20, 22, 21, 20 and 38 mm, respectively. Meanwhile, CMC/St@ZnONPs composite displayed antimicrobial activity higher than monometallic ZnONPs where inhibition zones were 40, 25, 43, 17, 25, 25, 25 and 45 mm against *k. pneumonia* 124, *K. pneumonia* 117, *B. subtilis*, *K. pneumonia* 115, *Acinetobacter bumanii* 110, *pseudomonas aerogenosa*, *E. coli* 127, *C. albicans*.

Table 1. Isolated pathogenic bacteria and *Candida*; number and frequency.

Microbial strains	Number	Isolation frequency (%)
<i>Candida albicans</i>	1	3.33
<i>Aeromonas veronii</i>	1	3.33
<i>Bacillus subtilis</i>	1	3.33
<i>Citrobacter youngae</i>	1	3.33
<i>Klebsiella ozaenae</i>	1	3.33
<i>Proteus mirabilis</i>	1	3.33
<i>Pseudomonas aeruginosa</i>	1	3.33
<i>Pseudomonas fluorescens</i>	1	3.33
<i>Serratia marcescens</i>	1	3.33
<i>Staphylococcus heamolyticus</i>	1	3.33
<i>Enterobacter cloacae</i>	2	6.67
<i>Acinetobacter baumannii</i>	3	10
<i>Escherichia coli</i>	5	16.67
<i>Klebsiella pneumonia</i>	10	33.33
Total	30	100

On the other hand, zinc acetate as a start material had weak antimicrobial activity toward some of the tested bacterial and fungal isolates.

The antimicrobial mechanisms of carboxymethyl cellulose CMC/St@ZnONPs nanoparticles (ZnONPs) composites primarily involve the physical and chemical interactions between the composite material and microbial cells. ZnO nanoparticles possess intrinsic properties that can disrupt microbial cell membranes, leading to cell leakage and ultimately cell death. When incorporated into the CMC-starch matrix, these nanoparticles enhance the composite's surface area and reactivity (Siddiqi et al. 2018, Irede et al. 2024). The presence of CMC and starch not only provides a biocompatible environment but also can facilitate the sustained release of ZnO ions, which further contributes to the antimicrobial activity by generating reactive oxygen species (ROS). These ROS can damage cellular components, including lipids, proteins, and DNA, effectively hindering microbial growth and proliferation (Zhong et al. 2018).

Previous studies reported the antimicrobial activity of nanocomposites based on ZnONPs. (Shehabeldine et al. (2022) reported that cotton fabrics with nanocomposite based on ZnONPs acyclovir, nanochitosan, and clove oil showed promising antibacterial activity toward *S. aureus*, *S. pyogenes*, *E. coli* and *K. aerogenes*. (Hasanin et al. (2023c) succeeded in the preparation of nanocomposite based on mycosynthesized bimetallic Zn-CuO NPs, nanocellulose, and chitosan, where this nanocomposite had antimicrobial activity toward *B. subtilis*, *E. coli* and *S. aureus*, *C. albicans* and *C. neoformans*.

***In vitro* cytotoxicity of ZnONPs and CMC/St@ZnONPs nanocomposite**

The potential cytotoxic effect of ZnONPs and CMC/St@ZnONPs composites was evaluated against Vero normal cell line to determine the maximum non-toxic dose (MNTD). As shown in Figure 9, the viability of Vero cells was more than 88% with concentrations of 31.25, 62.5, and 125 $\mu\text{g mL}^{-1}$ for both ZnONPs and CMC/St@ZnONPs composite. The viability (%) of Vero cells were 99.4 ± 0.36 , 98.9 ± 0.97 , 95.5 ± 1.4 , 28.6 ± 1.0 , 8.6 ± 0.52 , and 3.15 ± 0.15 % corresponding to ZnONPs at concentrations 31.25, 62.5, 125, 250, 500, and 1000 $\mu\text{g mL}^{-1}$, respectively. Meanwhile, the viability (%) of Vero cells were 99.16 ± 0.29 , 98.3 ± 0.40 , 88.3 ± 1.25 , 24.7 ± 0.65 , 12.4 ± 0.68 , and 5.6 ± 0.6 % corresponding to CMC/St@ZnONPs composite at concentrations 31.25, 62.5, 125, 250, 500, and 1000 $\mu\text{g mL}^{-1}$, respectively. Furthermore, results illustrated that IC₅₀ of ZnONPs and CMC/St@ZnONPs toward Vero cells were 202.58 ± 2.19 and 193.94 ± 1.53 $\mu\text{g mL}^{-1}$, respectively. In general, if the IC₅₀ is ≥ 90 $\mu\text{g mL}^{-1}$, the material is classified as non-

cytotoxic (Ioset et al. 2009). Therefore, the biosynthesized ZnONPs and CMC/St@ZnONPs nanocomposite is considered safe to use.

***In vitro* anticancer activity of ZnONPs and CMC/St@ZnONPs nanocomposite**

Nanocomposites have emerged as promising materials in the field of cancer treatment due to their unique properties, such as enhanced surface area and the ability to encapsulate therapeutic agents. These composites often combine nanoparticles with polymers or other materials, allowing for targeted drug delivery, improved bioavailability, and reduced side effects (Mondal et al. 2023, Andoh and Ocansey 2024). In the current study, both ZnONPs and CMC/St@ZnONPs composite were evaluated anticancer activity toward MCF7 cancerous cell line as shown in Figure 10. Results showed that the exposure of MCF7 (human breast cancer cell) to effect of ZnONPs and CMC/St@ZnONPs composite at various concentrations significantly reduced the cell viability in a concentration dependent manner. Results revealed that anticancer activity of ZnONPs at safe concentration 125, 62.5 and 31.25 $\mu\text{g mL}^{-1}$ were 83.21, 52.52 and 0.17 % respectively. Moreover, CMC/St@ZnONPs composite showed anticancer activity but slightly lower than ZnONPs only, where were 73.4, 47.87 and 0 % toward MCF7 cell line as shown in Figure 10. Additionally, IC₅₀ of both ZnONPs and CMC/St@ZnONPs composite against MCF7 were 61.22 ± 1.09 and 84.47 ± 2.48 $\mu\text{g mL}^{-1}$.

Zinc oxide nanoparticles (ZnONPs) exhibit significant anticancer properties through various mechanisms, including the generation of reactive oxygen species (ROS), which can induce apoptosis in cancer cells. The incorporation of carboxymethyl cellulose (CMC) and starch to form a composite with ZnONPs enhances their stability and biocompatibility, allowing for targeted drug delivery and increased cellular uptake. This composite not only improves the therapeutic efficacy of ZnONPs but also minimizes side effects associated with conventional chemotherapy. Studies have shown that the CMC/St@ZnONPs composite can effectively inhibit tumor growth by promoting oxidative stress specifically in cancer cells while sparing normal cells, thereby paving the way for more effective cancer treatments (Bisht and Rayamajhi 2016).

Conclusion

In conclusion, the study successfully demonstrated the mycosynthesis of zinc oxide nanoparticles (ZnONPs) and their composite with CMC-Starch, highlighting their

Table 2: Antibiotic susceptibility profiles of the selected MDR pathogenic bacteria.

Antibiotics	<i>A. baumannii</i> 110		<i>B. subtilis</i>		<i>E. coli</i> 127		<i>K. pneumoniae</i> 115		<i>K. pneumoniae</i> 117		<i>K. pneumoniae</i> 124		<i>P. aeruginosa</i>	
	MIC	Index	MIC	Index	MIC	Index	MIC	Index	MIC	Index	MIC	Index	MIC	Index
Amikacin	>32	R	16	S	<=8	S	16	S	>32	R	>32	R	>32	R
Gentamicin	>8	R	>8	R	<=2	S	<=2	S	>8	R	>8	R	>8	R
Ertapenem	>4	R	>4	R	>4	R	>4	R	>4	R	>4	R	>4	R
Imipenem	>8	R	>8	R	8	R	>8	R	>8	R	>8	R	>8	R
Meropenem	>8	R	>8	R	8	R	>8	R	>8	R	>8	R	>8	R
Cephalothin	>16	R	>16	R	>16	R	>16	R	>16	R	>16	R	>16	R
Cefuroxime	>16	R	>16	R	>16	R	>16	R	>16	R	>16	R	>16	R
Cefoxitin	>16	R	>16	R	>16	R	>16	R	>16	R	>16	R	>16	R
Ceftazidime	>16	R	>16	R	>16	R	>16	R	>16	R	>16	R	>16	R
Ceftriaxone	>32	R	>32	R	>32	R	>32	R	>32	R	>32	R	>32	R
Cefepime	>16	R	>16	R	>16	R	>16	R	>16	R	>16	R	>16	R
Aztreonam	>16	R	>16	R	16	R	>16	R	>16	R	>16	R	>16	R
Ampicillin	>16	R	>16	R	>16	R	>16	R	>16	R	>16	R	>16	R
Amoxicillin-clavulanic acid (AMC)	>16/8	R	>16/8	R	>16/8	R	>16/8	R	>16/8	R	>16/8	R	>16/8	R
Piperacillin/ Tazobactam	>64/4	R	>64/4	R	>64/4	R	>64/4	R	>64/4	R	>64/4	R	>64/4	R
Trimethoprim/sulfamethoxazole (SXT)	>4/76	R	<=1/19	S	>4/76	R	>4/76	R	<=1/19	S	>4/76	R	>4/76	R
Nitrofurantoin	>64	R	>64	R	<=16	S	>64	R	>64	R	>64	R	>64	R
Ciprofloxacin	>2	R	>2	R	>2	R	>2	R	>2	R	>2	R	>2	R
Levofloxacin	>4	R	>4	R	>4	R	>4	R	>4	R	>4	R	>4	R
Tigecycline	>4	R	>2	S	<=1	S	4	I	4	I	>2	S	>4	S

Where: The orange cells indicate (S) susceptibility to the tested antibiotic, the blue cells indicate (I) intermediate susceptibility to the tested antibiotic, and the unfilled cells indicate (R) resistance to the tested antibiotics.

Table 3. Antimicrobial activity of ZnONPs, CMC/St@ZnONPs and Zn(CH3COO)2.2H2O at concentration of 1000 µg mL⁻¹

Organism	Inhibition zone(mm)		
	ZnONPs	CMC/St@ZnONPs	Zinc acetate
<i>K. pneumonia</i> 124	28	40	0
<i>K. pneumonia</i> 117	21	25	7
<i>B. subtilis</i>	36	43	5
<i>C. albicans</i>	38	45	4
<i>K. pneumonia</i> 115	20	17	3
<i>A. bumanii</i> 110	22	25	0
<i>P. aerogenosa</i>	21	25	0
<i>E. coli</i> 127	20	25	3



Fig 8. Antimicrobial activity of ZnONPs, CMC/St@ZnONPs composites, and Zn (CH₃COO)₂.2H₂O using agar well diffusion method.

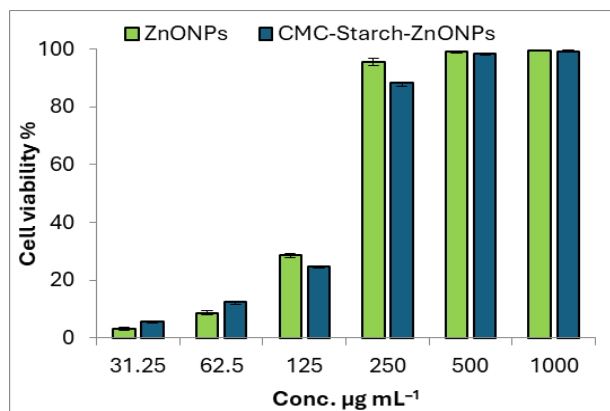


Fig 9. Effect of different concentrations of ZnONPs and CMC/St@ZnONPs nanocomposite toward Vero normal cell line.

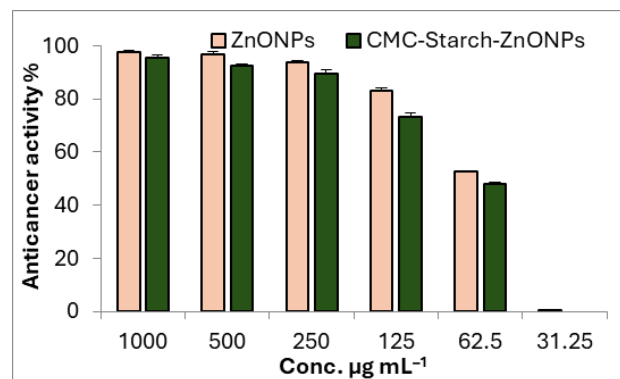


Fig 10. Anticancer activity of ZnONPs and CMC/St@ZnONPs nanocomposite toward MCF7 cancerous cell line at different concentrations.

potential as effective agents against multi-drug resistant pathogens. The antimicrobial assays showed that the CMC/St@ZnONPs nanocomposite exhibited superior activity against a range of resistant bacterial and fungal isolates, with notable inhibition zones. This suggests that such nanocomposites could serve as valuable alternatives in combating infections, particularly in an era where traditional antibiotics are becoming increasingly ineffective. Additionally, while ZnONPs showcased stronger anticancer activity against the MCF7 cell line compared to the composite, both materials exhibited promising results that warrant further investigation. As a consequence of the aforementioned findings, it may be inferred that *Rhizopus arrhizus* produces a variety of proteins and enzymes, obviating the need for chemical reducers and stabilizers. As a result, the biological method for the production of ZnONPs utilizing *Rhizopus arrhizus* has been presented in this work. The application of ZnONPs as antimicrobial and anticancer agents and their composites in has yet to be completely investigated and further study on risk assessment is still needed.

Acknowledgments

The authors express their sincere thanks to Faculty of Science (Boys), Al-Azhar University, Cairo, Egypt for providing the necessary research facilities. The authors would also like to acknowledge the facilities available at National Research Centre, Cairo, Egypt.

Conflict of interest

The authors declare that they have no conflict of interest.

References

- Abdel-Azeem A, Nada A, O'Donovan A, Thakur VK, Elkelish A. (2020). Mycogenic Silver Nanoparticles from Endophytic *Trichoderma atroviride* with Antimicrobial Activity. *Journal of Renewable Materials*, 8(2): 171-185.
- Abdelraof M, Ibrahim S, Selim M, Hasanin M. (2020). Immobilization of L-methionine γ -lyase on different cellulosic materials and its potential application in green-selective synthesis of volatile sulfur compounds *Journal of Environmental Chemical Engineering*, 8(4): 103870.
- Abu-Elghait M, Hasanin M, Hashem A H, Salem SS. (2021). Ecofriendly novel synthesis of tertiary composite based on cellulose and myco-synthesized selenium nanoparticles: Characterization, antibiofilm and biocompatibility. *International Journal of Biological Macromolecules*, 175: 294-303.
- Al-Askar AA, Hashem AH, Elhussieny NI, Saied E. (2023). Green Biosynthesis of Zinc Oxide Nanoparticles Using *Pluchea indica* Leaf Extract: Antimicrobial and Photocatalytic Activities. *Molecules* 28(12): 4679.
- Albalawi M A, Abdelaziz A M, Attia M S, Saied E, Elganzory H H, Hashem AH. (2022). Mycosynthesis of Silica Nanoparticles Using *Aspergillus niger*: Control of *Alternaria solani* Causing Early Blight Disease, Induction of Innate Immunity and Reducing of Oxidative Stress in Eggplant. *Antioxidants* 11(12): 2323.
- Almajidi Y Q, Gupta J, Sheri F S, Zabibah R S, A. Faisal, Ruzibayev A, Adil M, Saadh M J, Jawad M J, Alsaikhan F, Narmani A, Farhood B. (2023). Advances in chitosan-based hydrogels for pharmaceutical and biomedical applications: A comprehensive review. *International Journal of Biological Macromolecules* 253: 127278.
- Andoh V, Ocansey D K W. (2024). The Advancing Role of Nanocomposites in Cancer Diagnosis and Treatment. *International Journal of Nanomedicine*, 19: 6099-6126.
- Bisht G, Rayamajhi S. (2016). ZnO Nanoparticles: A Promising Anticancer Agent. *Nanobiomedicine (Rij)* 3: 9.
- Cong Z, Tran O, Nelson J, Silver M, Chung K. (2022). Productivity Loss and Indirect Costs for Patients Newly Diagnosed with Early- versus Late-Stage Cancer in the USA: A Large-Scale Observational Research Study. *Appl Health Econ Health Policy* 20(6): 845-856.
- El-Khawaga A M, Elsayed M A, Gobara M, Suliman A A, Hashem A H, Zaher A A, Mohsen M, Salem S S. (2023). Green synthesized ZnO nanoparticles by *Saccharomyces cerevisiae* and their antibacterial activity and photocatalytic degradation. *Biomass Conversion and Biorefinery* 15(2): 2673-2684.
- Elbasuney S, El-Sayyad G S, Tantawy H, Hashem A H. (2021). Promising antimicrobial and antibiofilm activities of reduced graphene oxide-metal oxide (RGO-NiO, RGO-AgO, and RGO-ZnO) nanocomposites. *RSC advances* 11(42): 25961-25975.
- Elkady F M, Hashem A H, Salem S S, El-Sayyad G S, Tawab A A, Alkherkhis M M, Abdulrahman M S. (2024). Unveiling biological activities of biosynthesized starch/silver-selenium nanocomposite using *Cladosporium cladosporioides* CBS 174.62. *BMC Microbiology* 24(1): 78.
- Elsayed N, Hasanin M S, Abdelraof M. (2022). Utilization of olive leaves extract coating incorporated with zinc/selenium oxide nanocomposite to improve the postharvest quality of green beans pods. *Bioactive Carbohydrates and Dietary Fibre* 28: 100333.
- Fouda A, Khalil A, El-Sheikh H, Abdel-Rhman E, Hashem A. (2015). Biodegradation and detoxification of bisphenol-A by filamentous fungi screened from nature. *Journal of Advances in Biology & Biotechnology*: 123-132.
- Gaber S E, Hashem A H, El-Sayyad G S, Attia M S. (2024). Antifungal activity of myco-synthesized bimetallic ZnO-CuO nanoparticles against fungal plant pathogen *Fusarium oxysporum*. *Biomass Conversion and Biorefinery* 14(20): 25395-25409.
- Gopinath V, Kamath S M, Priyadarshini S, Chik Z, Alarfaj A A, Hirad A H. (2022). Multifunctional applications of natural polysaccharide starch and cellulose: An update on recent advances. *Biomedicine and pharmacotherapy* 146: 112492.
- Hasanin M, Abdel Kader A H, Abd El-Sayed E S, Kamel S. (2023). Green Chitosan-Flaxseed Gum Film Loaded with ZnO for Packaging Applications. *Starch-Stärke*:75(5-6), 2200132.
- Hasanin M., Al Abboud M A, Alawlaqi M M, Abdelghany T M, Hashem A H. (2022). Ecofriendly Synthesis of Biosynthesized Copper Nanoparticles with Starch-Based Nanocomposite: Antimicrobial, Antioxidant, and Anticancer Activities. *Biological Trace Element Research* 200(5): 2099-2112.
- Hasanin M, Elbahnasawy M A, Shehabeldine A M, Hashem A H. (2021). Ecofriendly preparation of

- silver nanoparticles-based nanocomposite stabilized by polysaccharides with antibacterial, antifungal and antiviral activities. *BioMetals* 34(6): 1313-1328.
- Hasanin M, Hashem A H, Lashin I, Hassan S A. (2023). In vitro improvement and rooting of banana plantlets using antifungal nanocomposite based on myco-synthesized copper oxide nanoparticles and starch. *Biomass Conversion and Biorefinery* 13(10): 8865-8875.
- Hasanin M, Taha N F, Abdou A R, Emara L H. (2022). Green decoration of graphene oxide Nano sheets with gelatin and gum Arabic for targeted delivery of doxorubicin. *Biotechnology Reports* 34: e00722.
- Hasanin M S. (2021). Simple, economic, ecofriendly method to extract starch nanoparticles from potato peel waste for biological applications. *Starch-Stärke*: 37(9-10), 2100055.
- Hasanin M S, Hashem A H, Abd El-Sayed E S, El-Saied H. (2020). Green ecofriendly bio-deinking of mixed office waste paper using various enzymes from *Rhizopus microsporus* AH3: efficiency and characteristics. *Cellulose*: 27, (4443-4453).
- Hasanin M S, Hashem A H, Al-Askar A A, Haponiuk J, Saied E. (2023). A novel nanocomposite based on mycosynthesized bimetallic zinc-copperoxide nanoparticles, nanocellulose and chitosan: characterization, antimicrobial and photocatalytic activities. *Electronic Journal of Biotechnology* 65: 45-55.
- Hasanin M S, Youssef A M. (2022). Ecofriendly bioactive film doped CuO nanoparticles based biopolymers and reinforced by enzymatically modified nanocellulose fibers for active packaging applications. *Food Packaging and Shelf Life* 34: 100979.
- Hashem AH, El-Sayyad GS. (2024). Antimicrobial and anticancer activities of biosynthesized bimetallic silver-zinc oxide nanoparticles (Ag-ZnO NPs) using pomegranate peel extract. *Biomass Conversion and Biorefinery* 14(17): 20345-20357.
- Hashem A H, Hasanin M S, Khalil A M A, Suleiman WB. (2019). Eco-green conversion of watermelon peels to single cell oils using a unique oleaginous fungus: *Lichtheimia corymbifera* AH13. *Waste and Biomass Valorization*: 11-5721-5732.
- Hashem A H, Al-Askar A A, Saeb M R, Abd-Elsalam K A, El-Hawary A S, Hasanin M. S. (2023a). Sustainable biosynthesized bimetallic ZnO@ SeO nanoparticles from pomegranate peel extracts: antibacterial, antifungal and anticancer activities. *RSC advances* 13(33): 22918-22927.
- Hashem A H, El-Sayyad G S, Al-Askar A A, Marey S AbdElgawad H, Abd-Elsalam K A, Saied E. (2023b). Watermelon Rind Mediated Biosynthesis of Bimetallic Selenium-Silver Nanoparticles: Characterization, Antimicrobial and Anticancer Activities. *Plants* 12(18): 3288.
- Hashem AH, Rizk SH, Abdel-Maksoud MA, Al-Qahtani WH, AbdElgawad H, El-Sayyad GS. (2023c). Unveiling anticancer, antimicrobial, and antioxidant activities of novel synthesized bimetallic boron oxide-zinc oxide nanoparticles. *RSC advances* 13(30): 20856-20867.
- Hashem A H, Saied E, Ali O M, Selim S, Al Jaouni S K, Elkady F M, El-Sayyad G S. (2023d). Pomegranate Peel Extract Stabilized Selenium Nanoparticles Synthesis: Promising Antimicrobial Potential, Antioxidant Activity, Biocompatibility, and Hemocompatibility. *Applied Biochemistry and Biotechnology* 195(10): 5753-5776.
- Hashem A H, Suleiman W B, Abu-elreesh G, Shehabeldine A M, Khalil A M A. (2020). Sustainable lipid production from oleaginous fungus *Syncephalastrum racemosum* using synthetic and watermelon peel waste media." *Bioresource Technology Reports* 12: 100569.
- Hashem A H, Suleiman W B, Abu-Elrish G M, El-Sheikh H H. (2020). Consolidated Bioprocessing of Sugarcane Bagasse to Microbial Oil by Newly Isolated Oleaginous Fungus: *Mortierella wolfii*. *Arabian Journal for Science and Engineering*: 46, 199-211.
- Hocking L, Ali G C, d'Angelo C, Deshpande A, Stevenson C, Virdee M., Guthrie S. (2021). A rapid evidence assessment exploring whether antimicrobial resistance complicates non-infectious health conditions and healthcare services, 2010-20. *JAC Antimicrob Resist* 3(4): dlab171.
- Ioset J R, Brun R, Wenzler T, Kaiser M, Yardley V. (2009). Drug screening for kinetoplastids diseases. A Training Manual for Screening in Neglected Diseases. DNDi and Pan-Asian Screening Network, 74pp.
- Irede E L, Awoyemi R F, Owolabi B., Aworinde O R, Kajola O, Hazeez A, Raji A. A., Ganiyu L O, Onukwuli C O, Onivefu A P, Ifijen I H. (2024). Cutting-edge developments in zinc oxide nanoparticles: synthesis and applications for enhanced antimicrobial and UV protection in healthcare solutions. *RSC Advances* 14(29): 20992-21034.
- Kader M A, Shahruzzaman M, Parvin N, Shams K, Kamruzzaman M, Haque P, Khan M A. (2024). Development of biocompatible packaging material:

- starch/PVA-based bio-composite enhanced with hydroxypropyl methylcellulose. *Polymer-Plastics Technology and Materials* 63(17): 2418-2432.
- Kamel, A, Suleiman W B, Elfeky A, El-Sherbiny G M, Elhaw M. (2022). Characterization of bee venom and its synergistic effect combating antibiotic resistance of *Pseudomonas aeruginosa*. *Egyptian Journal of Chemistry* 65(5): 297-306.
- Karam S T, Abdulrahman A F (2022). Green synthesis and characterization of ZnO nanoparticles by using thyme plant leaf extract. *Photonics* 9 (8):594.
- Khalil A M A, Hashem A H. (2018). Morphological changes of conidiogenesis in two *Aspergillus* species. *J Pure Appl Microbiol* 12(4): 2041-2048.
- Khalil A M A, Hashem A H, Abdelaziz AM. (2019). Occurrence of toxigenic *Penicillium polonicum* in retail green table olives from the Saudi Arabia market. *Biocatalysis and Agricultural Biotechnology* 21: 101314.
- Kim K H, Yoshihara Y, Abe Y, Kawamura M, Kiba T. (2017). Morphological characterization of sphere-like structured ZnO-NiO nanocomposites with annealing temperatures. *Materials Letters* 186: 364-367.
- Kumar H, Rani R. (2013). Structural and optical characterization of ZnO nanoparticles synthesized by microemulsion route. *International Letters of Chemistry, Physics and Astronomy* 19(14):22-36.
- Kumar N R, Balraj T A, Kempegowda S N, Prashant A. (2024). Multidrug-Resistant Sepsis: A Critical Healthcare Challenge. *Antibiotics* 13(1):46.
- López C, Rodríguez-Paez J E. (2017). Synthesis and characterization of ZnO nanoparticles: effect of solvent and antifungal capacity of NPs obtained in ethylene glycol. *Applied Physics A* 123(12): 748.
- Mondal A, Nayak A K, Chakraborty P. (2023). Natural Polymeric Nanobiocomposites for Anti-Cancer Drug Delivery Therapeutics: A Recent Update. 15(8): *Pharmaceutics* 2064.
- Muteeb G, Rehman M T. (2023). Origin of Antibiotics and Antibiotic Resistance, and Their Impacts on Drug Development: A Narrative Review. *Antibiotics* 16(11), 1615.
- Neal R D, Tharmanathan P, France B, Din N U, Cotton S, Fallon-Ferguson J, Hamilton W, Hendry A M, Lewis R, Macleod U, Mitchell E D, Pickett M., Rai T, Shaw K, Stuart N, Tørring M L, Wilkinson C, Williams B, Williams N, Emery J. (2015). Is increased time to diagnosis and treatment in symptomatic cancer associated with poorer outcomes? Systematic review. *Br J Cancer* 112 Suppl 1(Suppl 1): S92-107.
- Pourmadadi M, Rahmani E, Shamsabadipour A, Samadi A, Esmaeili J, Arshad R, Rahdar A, Tavangarian F, Pandey S. (2023). Novel carboxymethyl cellulose based nanocomposite: A promising biomaterial for biomedical applications. *Process Biochemistry* 130: 211-226.
- Reddy G K, Reddy A J, Krishna R H, Nagabhushana B, Gopal G R. (2017). Luminescence and spectroscopic investigations on Gd³⁺ doped ZnO nanophosphor. *Journal of Asian Ceramic Societies* 5(3): 350-356.
- Ruddaraju L K, Pammi S, Pallela P V K, Padavala V S, Kolapalli V R M. (2019). Antibiotic potentiation and anti-cancer competence through bio-mediated ZnO nanoparticles. *Materials Science and Engineering: C* 103: 109756.
- Saied E, Hashem A H, Ali O M, Selim S, Almuhayawi M S, Elbahnasawy M A. (2022). Photocatalytic and Antimicrobial Activities of Biosynthesized Silver Nanoparticles Using *Cytobacillus firmus*. *Life* 12(9): 1331.
- Saied M, Hasanin M, Abdelghany T M, Amin B H, Hashem A H. (2023). Anticandidal activity of nanocomposite based on nanochitosan, nanostarch and mycosynthesized copper oxide nanoparticles against multidrug-resistant *Candida*. *International Journal of Biological Macromolecules* 242: 124709.
- Salam M A, Al-Amin M Y, Salam M T, Pawar J S, Akhter N. (2023). Antimicrobial Resistance: A Growing Serious Threat for Global Public Health. *Healthcare* 11(13): 1946.
- Samir M, Al Kiey S A, Rokbaa H H, El-Sherbiny S, Hasanin M S. (2024). Innovative Ag@ Cu/white sand and polysaccharide based nanocomposites: A simple route to conductive and antibacterial paper coatings. *Materials Chemistry and Physics*: 328, 129974.
- Saravanan H, Subramani T, Rajaramon S, David H., Sajeevan A., Sujith S., A. Solomon P. (2023). Exploring nanocomposites for controlling infectious microorganisms: charting the path forward in antimicrobial strategies. *Front Pharmacol* 14: 1282073.
- Shawky M, Suleiman W B, Farrag A A. (2021). Antibacterial Resistance Pattern in Clinical and Non-clinical Bacteria by Phenotypic and Genotypic Assessment. *Journal of Pure and Applied Microbiology* 15(4).
- Shehabeldine A M, Hashem A H, Wassel A R, Hasanin M. (2022). Antimicrobial and Antiviral Activities of Durable Cotton Fabrics Treated with Nanocomposite Based on Zinc Oxide

- Nanoparticles, Acyclovir, Nanochitosan, and Clove Oil. *Applied Biochemistry and Biotechnology* 194(2): 783-800.
- Shrestha S, Wang B, Dutta P. (2020). Nanoparticle processing: Understanding and controlling aggregation. *Advances in colloid and interface science* 279: 102162.
- Siddiqi K S, Rahman A Ur, Tajuddin, A. Husen. (2018). Properties of Zinc Oxide Nanoparticles and Their Activity Against Microbes. *Nanoscale Research Letters* 13(1): 13.
- Smith G L, Lopez-Olivo M A, Advani P G, Ning M S, Geng Y, Giordano S H, Volk R J. (2019). Financial Burdens of Cancer Treatment: A Systematic Review of Risk Factors and Outcomes. *J Natl Compr Canc Netw* 17(10): 1184-1192.
- Soliman M O, Suleiman W B, Roushdy M M, Elbatrawy E N, Gad A M. (2022). Characterization of some bacterial strains isolated from the Egyptian Eastern and Northern coastlines with antimicrobial activity of *Bacillus zhangzhouensis* OMER4. *Acta Oceanologica Sinica* 41(3): 86-93.
- Soubhagya, A, Balagangadharan K, Selvamurugan N, Sathya Seeli D, Prabakaran M. (2022). Preparation and characterization of chitosan/carboxymethyl pullulan/bioglass composite films for wound healing. *Journal of Biomaterials Applications* 36(7): 1151-1163.
- Srivastava S, Usmani Z, Atanasov AG, Singh VK, Singh NP, Abdel-Azeem AM, Prasad R, Gupta G, Sharma M, Bhargava A. (2021). Biological Nanofactories: Using Living Forms for Metal Nanoparticle Synthesis. *Mini-Reviews in Medicinal Chemistry*, 21, 245-265
- Turky G, Moussa M A, Hasanin M, El-Sayed N S, Kamel S. (2020). Carboxymethyl Cellulose-Based Hydrogel: Dielectric Study, Antimicrobial Activity and Biocompatibility. *Arabian Journal for Science and Engineering*: 46, 17-30.
- Van de Loosdrecht A, Beelen R, Ossenkoppele G, Broekhoven M, Langenhuijsen M. (1994). A tetrazolium-based colorimetric MTT assay to quantitate human monocyte mediated cytotoxicity against leukemic cells from cell lines and patients with acute myeloid leukemia. *J Immunol Methods* 174(1-2): 311-320.
- Visagie C, Houbraken J, Frisvad J C, Hong S-B., Klaassen C, Perrone G, Seifert K, Varga J, Yaguchi T, Samson R. (2014). Identification and nomenclature of the genus *Penicillium*. *Studies in mycology* 78(1): 343-371.
- Więckiewicz G, Weber S, Florczyk I. (2024). Socioeconomic Burden of Psychiatric Cancer Patients: A Narrative Review. *Cancers* 16(6), 1108.
- Zaki S A, Ouf S A, Albarakaty F M, Habeb M M, A A Aly, Abd-Elsalam K A. (2021). "Trichoderma harzianum-mediated ZnO nanoparticles: A green tool for controlling soil-borne pathogens in cotton. *Journal of Fungi* 7(11): 952.
- Zhong Q, Tian J, Liu T, Guo Z, Ding S, Li H. (2018). Preparation and antibacterial properties of carboxymethyl chitosan/ZnO nanocomposite microspheres with enhanced biocompatibility. *Materials Letters* 212: 58-61.